


RESEARCH ARTICLE

Volume-rendered optical coherence tomography angiography during ocular interventions: Advocating for noninvasive intraoperative retinal perfusion monitoring

Tim J. Enz^{1,2,3}  | Peter M. Maloca^{1,4,5} | Markus Tschopp^{3,6} |
Marcel N. Menke^{3,6} | James R. Tribble² | Pete A. Williams² | Nadja Inglin⁴ |
Ulrike Steitz³ | Hendrik P. N. Scholl^{1,4} | Anthia Papazoglou³

¹Department of Ophthalmology,
University of Basel, Basel, Switzerland

²Department of Clinical Neuroscience,
Division of Eye and Vision, St. Erik Eye
Hospital, Karolinska Institutet,
Stockholm, Sweden

³Department of Ophthalmology, Cantonal
Hospital Aarau, Aarau, Switzerland

⁴Institute of Molecular and Clinical
Ophthalmology Basel, Basel, Switzerland

⁵Moorfields Eye Hospital NHS
Foundation Trust, London, UK

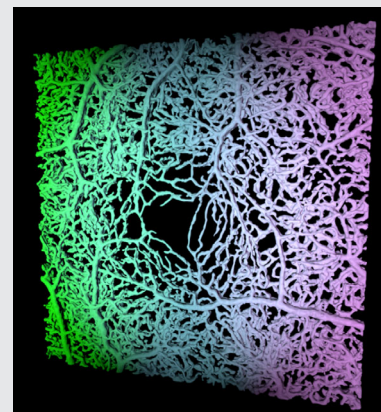
⁶Department of Ophthalmology,
Inselspital, Bern University Hospital,
University of Bern, Bern, Switzerland

Correspondence

Tim J. Enz, Department of
Ophthalmology, University of Basel,
Basel, 4031, Switzerland.
Email: tim.enz@aol.com

Abstract

We aimed to test for feasibility of volume-rendered optical coherence tomography angiography (OCTA) as a novel method for assessing/quantifying retinal vasculature during ocular procedures and to explore the potential for intraoperative use. Thirty patients undergoing periocular anaesthesia were enrolled, since published evidence suggests a reduction in ocular blood flow. Retinal perfusion was monitored based



on planar OCTA image-derived data provided by a standard quantification algorithm and postprocessed/volume-rendered OCTA data using a custom software script. Overall, imaging procedures were successful, yet imaging artifacts occurred frequently. In interventional eyes, perfusion parameters decreased during anaesthesia. Planar image-derived and volume rendering-derived parameters were correlated. No correlation was found between perfusion parameters and a motion artifact score developed for this study, yet all perfusion parameters correlated with signal strength as displayed by the device. Concluding, volume-rendered OCTA allows for noninvasive three-dimensional retinal vasculature assessment/quantification in challenging surgical settings and appears generally feasible for intraoperative use.

Abbreviations: 2D, two-dimensional; 3D, three-dimensional; BP, blood pressure; FA, fluorescence angiography; FoMA score, Free-of-motion-artifact score; iOCT, intraoperative optical coherence tomography; IOP, intraocular pressure; OCT, optical coherence tomography; OCTA, optical coherence tomography angiography.

Tim J. Enz and Peter M. Maloca contributed equally to this study.

This is an open access article under the terms of the [Creative Commons Attribution-NonCommercial-NoDerivs](https://creativecommons.org/licenses/by-nc-nd/4.0/) License, which permits use and distribution in any medium, provided the original work is properly cited, the use is non-commercial and no modifications or adaptations are made.

© 2022 The Authors. *Journal of Biophotonics* published by Wiley-VCH GmbH.

KEYWORDS

3D vasculature reconstruction, intraoperative, retinal perfusion monitoring, retinal vessel size, volume-rendered optical coherence tomography angiography

1 | INTRODUCTION

Intraoperative retinal vasculature assessment using fluorescence angiography (FA) has been tested for various clinical indications, including localization of retinal neovascularization or delineation of avascular retina. [1, 2] Recent evidence supports particularly three-dimensionally (3D) visualized FA for clinical use.[3, 4] However, intraoperative applicability of FA is limited given the complicated arrangement, invasiveness, associated risks, side effects, and the lack of objective/automated vessel quantification, calling for alternative and more feasible techniques that lend themselves to be utilized day-to-day in the clinic.

In contrast, optical coherence tomography angiography (OCTA) is a noninvasive imaging method used for assessing the retinal vasculature, based on the analysis of temporal changes in laser light reflectance of the surface of scattering particles. [5–8] While OCTA has replaced FA in many nonsurgical settings, [9] and although conventional optical coherence tomography (OCT) without angiography has established itself as a useful intraoperative tool (iOCT), [10] the potential of OCTA for intraoperative retinal vasculature assessment has only begun to be explored. An obstacle with current techniques, as a compromise between the vast amount of data and the limited capacities for their visual illustration, OCTA images are usually displayed in two-dimensions (2D; *en face*). As a result of this simplification, retinal vessels are only partially depicted as they exist in a 3D space. [5] On the other hand, OCTA offers advantages over FA in terms of automated and objective vasculature assessment, since many OCTA devices provide built-in quantification software. AngioPlex Metrix for example, the standard angiography analysis software in Zeiss Cirrus OCTA devices, calculates perfusion density, which represents the number of pixels with perfused vasculature divided by the total number of pixels in a given retinal region of measurement (expressed as a percentage of the respective OCTA image). [11] Perfusion density is affected by vessel size and therefore allows for conclusions regarding changes in retinal vessel calibres (e.g., vasoconstriction). However, as these quantification algorithms are based on 2D data, the results are only a vague approximation to reality.

Recently, visualization of imaging information has been enhanced by volume-rendering of OCTA data to

display spatial 3D vessel models. [12] Volume-rendering of OCTA data preserves the 3D relationship between the retinal vascular layers and hence allows for visualization of the retinal vasculature in much greater detail. [13] These 3D vessel models can be further analyzed for measuring vessel surface area and vessel volume, enabling quantification and characterization of the macular vasculature at the micron-level in unprecedented detail. [14, 15] It is reasonable to assume that this is currently the most advanced OCTA-based retinal vessel quantification method. Theoretically, this technology not only allows for 3D retinal vasculature assessment, but also for monitoring small changes in retinal vessel calibres during ocular procedures. Previously, this method has only been used for assessing and quantifying retinal vasculature in static conditions of long-standing retinal vessel alterations in nonsurgical clinical outpatient settings (diabetic retinopathy, Stargardt Disease) and not intraoperatively or for short-term changes. [14, 15]

Retinal ischemia is a poorly understood complication in ocular surgery and periocular anaesthesia. [16] Intraoperative and postoperative retinal vaso-occlusion has been described, sometimes with permanent visual sequelae. [17–27] Multiple lines of evidence suggest that periocular anaesthetic procedures cause a decrease in ocular blood flow, possibly leading to retinal ischemia [28–30], although the mechanism behind this phenomenon remains unclear. [16, 20] It is hypothesized that the anaesthetics exert a pharmacological vaso-constrictive effect, thereby diminishing retinal blood supply. [24, 27, 31, 32] The study presented here aims to test for feasibility of volume-rendered OCTA for 3D assessment of the retinal vasculature and quantification of retinal vessel calibres at the micron-level under real-life conditions of surgical procedures, and to explore its potential for intraoperative use. To this purpose, we enrolled patients undergoing periocular anaesthesia, since evidence suggests retinal vasoconstriction and reduction in retinal blood flow.

2 | METHODS

This observational study was conducted in accordance with the Declaration of Helsinki and was approved by the competent ethics committee (Ethikkommission Nordwest- und Zentralschweiz, 2019-01689). Written informed consent was obtained from all patients.

2.1 | Inclusion Criteria and patient characteristics

Thirty patients undergoing phacoemulsification cataract surgery under local anaesthesia were enrolled. Only patients without signs and history of retinal or optic nerve diseases were included, as assessed upon the preoperative visit including ophthalmoscopy and OCT of the macula and the optic disc. Sixteen patients were female. The age range was 59–86 years (mean 73.8 ± 7.06 [\pm SD] years). Nineteen patients had their right eye and 11 patients had their left eye operated on. The eyes that were to be operated on formed the interventional group, while the fellow eyes served as controls.

2.2 | Sub-Tenon's anaesthesia and imaging procedures

Both pupils of all enrolled patients were dilated with three tropicamide 0.5% and phenylephrine 5% eye drops on each side. IOP was measured using a portable Icare pro tonometer (Icare Finland, Oy, Vantaa Finland) and arterial blood pressure (BP) was assessed using a Mindray VS800 Vital Signs Monitor (Mindray Medical International, Shenzhen, China). A series of OCTA (Spectral-Domain Cirrus HD-OCT 5000, Carl Zeiss Meditec, Dublin, USA) volumes of the central macula (3x3x2mm) was obtained from each eye over a period of approximately 25 min. Then, on the interventional side, the ocular surface was anaesthetized with Tetracaine 1% eye drops. The periocular area was carefully cleaned and the ocular surface was disinfected with povidone-iodine solution 5% for 90 s. The patients were asked to gaze up and to the side and a small incision in the conjunctiva and Tenon's capsule was performed in the inferomedial quadrant. The tissue was carefully dissected from the sclera using a blunt scissor. A syringe with a blunt cannula was inserted and advanced posteriorly behind the equator of the globe. Two millilitres of mepivacaine solution 2% were injected into the virtual space between the sclera and Tenon's capsule in proximity to the posterior pole. Subsequently, IOP in both eyes and arterial BP were measured, and another series OCTA images were taken on both eyes over a period of approximately 15 min. Images quality was judged by the investigators, taking into account image location, signal strength and artifacts. Only images considered of sufficient quality were used for postprocessing (see below).

2.3 | Image analysis, postprocessing and motion artifact assessment

Perfusion density parameters as provided by AngioPlex Metrix were retrieved from the device. Subsequently,

OCTA image raw data were exported from the device using the manufacturer's software. Postprocessing, volume-rendering and quantification of the images were conducted using custom software scripts written in Matlab R2017a (MathWorks Inc., Natick), as described in detail previously. [14, 15] Briefly, the contrast was optimized by contrast-limited adaptive histogram equalization and all images were sharpened using unsharp masking. Built-in Matlab functions were applied for these two steps. A "vesselness" filter was applied to enhance vessel structure, and "vesselness" per pixel was computed. Subsequently, the images were exported as single planar *en face* images and converted into binary files by hysteresis thresholding. The total of all binary files from one eye was merged into a 3D volume, based on which vessel surface area (μm^2) and vessel volume (μm^3) were calculated using integrated Matlab functions.

To assess the potential of 3D OCTA for monitoring retinal perfusion during ocular procedures by quantifying changes in retinal vessel size at the micron level and to demonstrate possible applications, we conducted three different analyses based on the collected image set: (a) averaged vessel data-based analysis; (b) time-standardized analysis and (c) image quality-oriented analysis. For better readability, vessel parameters are expressed in mm^2/mm^3 and rounded to one or two decimal places within this manuscript. The original numbers are presented in Table S1 to demonstrate capability of measurement at the micron-level.

To identify possible disruptive factors associated with the imaging process, the third data analysis involved a comparison with the conventional 2D vessel quantification algorithm and screening for correlations of perfusion parameters with differences in signal strength and imaging artifacts. For motion artifact assessment, images were graded according to the area affected by motion artifacts. Images completely free of artifacts equal a Free-of-Motion-Artifact score (FoMA score) of 4. If motion artifacts are present in approximately a fourth, half or three fourth of the image, FoMA score equals 3, 2 or 1, respectively. If motion artifacts are present all over the image, FoMA score equals 0.

2.4 | Statistical analysis

Changes in perfusion density, vessel surface area and vessel volume before versus during periocular anaesthesia were defined as primary outcomes. Motion artifacts, signal strength and changes in IOP and arterial BP were defined as secondary outcomes. All statistical analysis was performed in R (R Foundation for Statistical Computing, Vienna, Austria). Descriptive analysis with calculation of mean values and standard deviation was

performed. Data were tested for normality with a *Shapiro Wilk* test. Normally distributed data were compared by a paired Student's *t*-test. Nonnormally distributed data were transformed using squared transforms; data that remained nonnormally distributed was compared by a *Wilcoxon signed-rank* test. Correlations were assessed by a *Pearson's* correlation test or *Spearman's* rank correlation test for normally distributed and nonnormally distributed data, respectively. $P < 0.05$ was considered statistically significant. Unless otherwise stated, $*P < 0.05$, $**P < 0.01$, $***P < 0.001$. For box plots, the centre hinge represents the median with upper and lower hinges representing the first and third quartiles; whiskers represent 1.5 times the interquartile range. For the comparison between the interventional and the control group after sub-Tenon's block, post-hoc power calculation ($\alpha = 0.05$) revealed power of 88.5% for mean vessel surface area and power of 95.9% for mean vessel volume, implicating a minimum sample size of 25 and 21 patients, respectively.

3 | RESULTS

3.1 | Imaging procedures in surgical settings and volume-rendering of obtained data

Imaging procedures and postprocessing/volume-rendering of obtained data could be completed in all

patients. No complications or safety issues were reported. In each patient, a series of OCTA images was taken before and during periocular anaesthesia in both eyes (see Section 2). The number of images in each eye considered suitable for postprocessing, as judged by the investigators taking into account image location, signal strength and artifacts, was between 1 and 7 both before and during periocular anaesthesia (2–14 total). In the images used for postprocessing, the time interval between imaging and anaesthetic injection ranged from 2 to 29 min before and from 2 to 15 min following injection. Examples of 3D OCTA models of the macular vasculature of study subjects are shown in Figure 1.

3.2 | Quantitative analysis of 3D macular vasculature reconstruction of averaged and time-standardized data

In our first vessel size analysis, volume rendering-derived data from all available images before and after anaesthetic injection in each eye were averaged. Before, mean vessel surface area and volume were slightly lower in interventional eyes compared with controls (interventional: $37.87 \pm 8.8 \text{ mm}^2/0.15 \pm 0.04 \text{ mm}^3$; control: $41.33 \pm 11.5 \text{ mm}^2/0.17 \pm 0.01 \text{ mm}^3$; surface area $P = 0.086$; volume $P = 0.08$). Following periocular anaesthesia, vessel parameters were moderately higher in control eyes ($43.75 \pm 9.5 \text{ mm}^2/0.18 \pm 0.05 \text{ mm}^3$), while they decreased in treated eyes

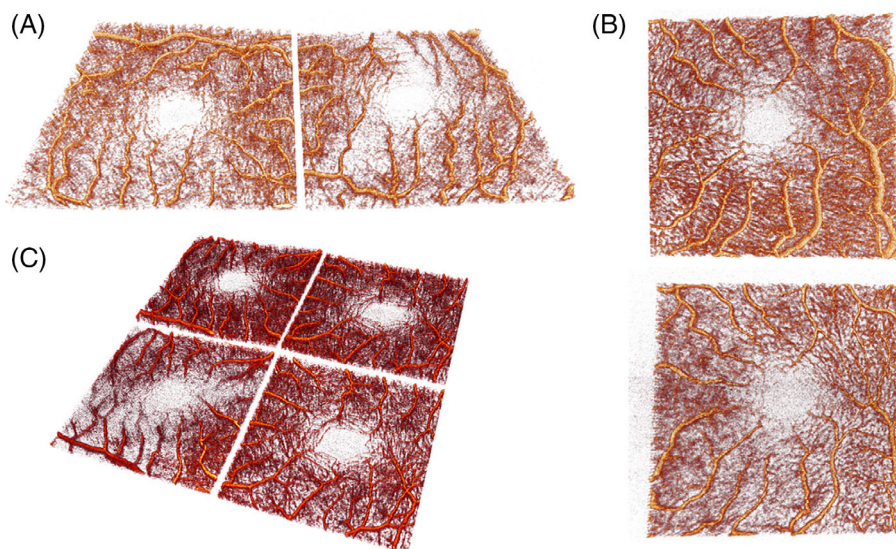


FIGURE 1 Three-dimensional OCTA vessel models of study subjects. Synoptic side view of 3D vessel models based on OCTA data of the right eye (left image) and the left eye (right image) of a study subject before application of sub-Tenon's block (A); *en face* view of 3D vessel models of the interventional left eye of another study subject with distinct vessel calibre changes; visualization of dilated (upper image) and constricted vessels (lower image) (B); skewed side view of 3D vessel models of the right (left column) and left (right column) eye before periocular anaesthesia (top row) and following periocular anaesthetic application (bottom row) of yet another study subject (C).

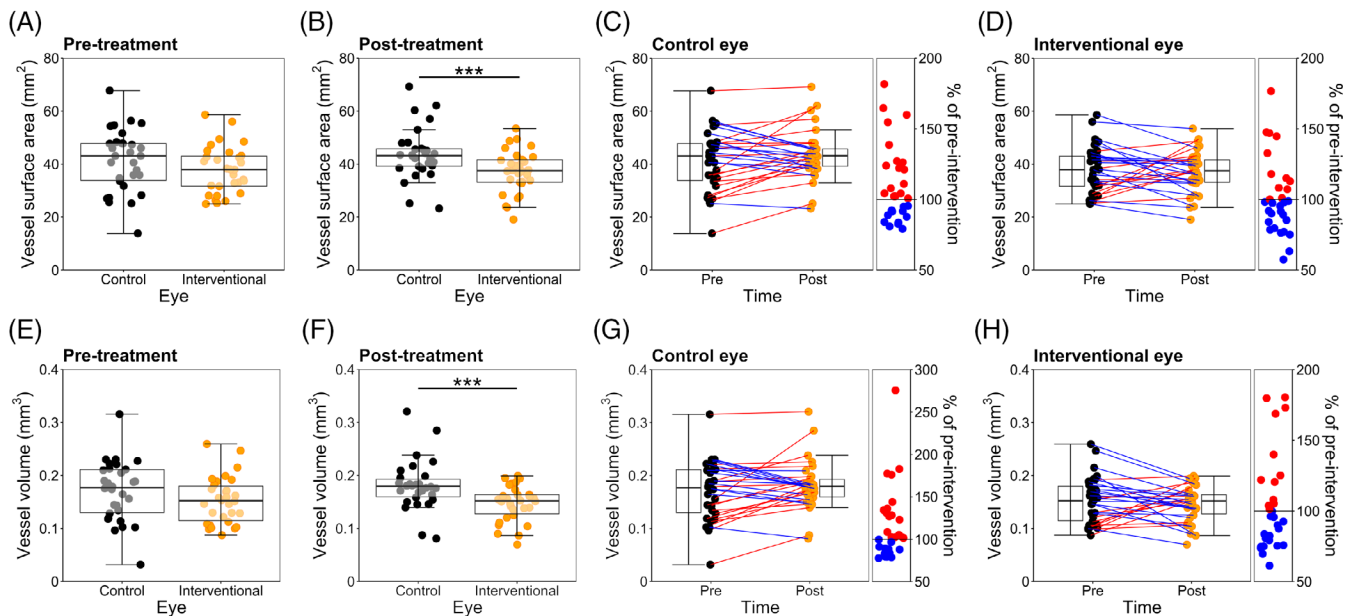


FIGURE 2 Averaged 3D vessel parameters in interventional eyes and control eyes before and after sub-Tenon's block. Box and whisker plots showing averaged vessel surface area (mm^2) in the control and interventional eyes before (A) and during (B) sub-Tenon's anaesthesia, as well as changes within the control (C) and the interventional group (D) before and following the anaesthetic block. Box and whisker plots showing averaged vessel volume (mm^3) in the control and interventional eyes before (E) and during (F) sub-Tenon's anaesthesia, as well as changes within the control (G) and the interventional group (H) before and following the anaesthetic block.

($37.11 \pm 7.9 \text{ mm}^2/0.14 \pm 0.03 \text{ mm}^3$). The postinterventional difference between the groups was significant (surface area $P < 0.001$; volume $P < 0.001$). Data are shown in Figure 2 and Table S1.

Averaged vessel surface area and volume was comparable in both groups before intervention, increased slightly in nontreated eyes after anaesthetic injection and decreased in the treated eyes.

A transient change in vessel parameters may be masked by the difference in the time over which images were acquired. To standardize measuring time-points, we performed further analysis using only one image before and during periorcular anaesthesia per eye. The pre-interventional images closest in time to the anaesthetic injection was selected, as well as the images as close as possible to the time-point 4 min afterwards (the time-point of maximum pharmacological effect). Before periorcular anaesthesia, mean total vessel surface and volume in the interventional and control groups were similar ($40.24 \pm 10.2 \text{ mm}^2/0.16 \pm 0.05 \text{ mm}^3$ and $42.13 \pm 11.2 \text{ mm}^2/0.17 \pm 0.05 \text{ mm}^3$, respectively; both $P = 0.28$). Following periorcular anaesthesia, in interventional eyes, both parameters decreased significantly ($35.83 \pm 8.99 \text{ mm}^2$, -10.95% , $P < 0.05$, 95% confidence interval [CI] -8.74 to -0.07 mm^2 ; $0.14 \pm 0.04 \text{ mm}^3$, -14.28% , $P < 0.05$, CI -0.04 to -0.002 mm^3), while remaining stable in control eyes ($43.49 \pm 9.5 \text{ mm}^2$, $+3.22\%$, $P = 0.40$; $0.18 \pm 0.05 \text{ mm}^3$, $+3.43\%$, $P = 0.57$). Comparing the two groups following periorcular anaesthesia, there was a

significant difference in both mean vessel surface area ($P < 0.001$) and mean vessel volume ($P < 0.001$). Data are shown in Figure 3 and Table S1.

Single volume-based vessel surface area and volume were similar in both groups before intervention, remained stable in nontreated eyes during periorcular anaesthesia, yet demonstrated a significant reduction in the treated eyes.

3.3 | Quantitative and qualitative analysis of perfusion density changes as provided by AngioPlex Metrix and comparison with 3D vessel size quantification

We next sought to expand the imaging modality and to screen for possible disruptive factors associated with the imaging process. To achieve this we conducted a third analysis selecting the images before and during the periorcular anaesthesia with the best quality in each patient, as judged by the investigators taking into account image location, signal strength and artifacts. We further added the conventional 2D vessel quantification method (measurement of perfusion density by AngioPlex Metrix) to the analysis, compared the results with those of the custom rendering-based measurements and screened for correlations between vessel parameters and imaging artifact occurrences.

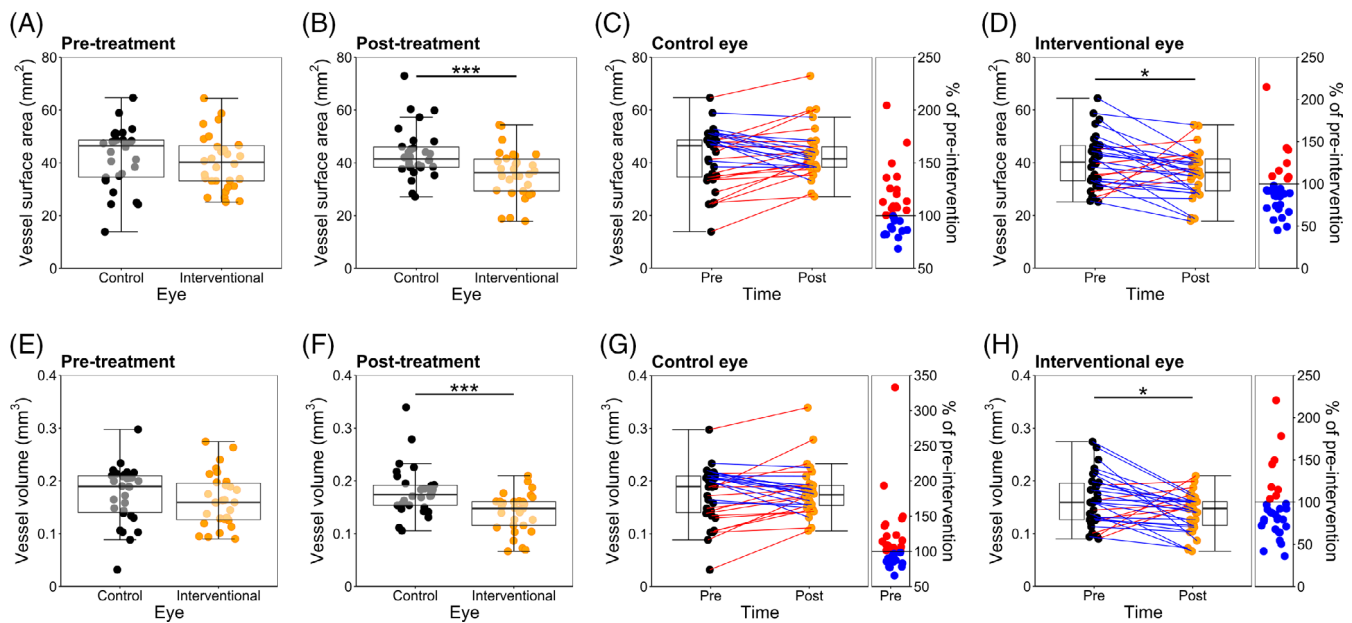


FIGURE 3 Time-standardized 3D vessel parameters in interventional eyes and control eyes before and after sub-Tenon's block. Top row: Box and whisker plots showing single-volume based vessel surface area (mm^2) in the control and interventional eyes before (A) and during (B) periocular anaesthesia, as well as changes within the control (C) and the interventional group (D) before and during periocular anaesthesia. Bottom row: Box and whisker plots showing single-volume based vessel volume (mm^3) in the control and interventional eyes before (E) and during (F) periocular anaesthesia, as well as changes within the control (G) and the interventional group (H) before and during periocular anaesthesia.

3.3.1 | 2D/3D retinal perfusion parameters

In this third dataset, before periocular anaesthesia, mean perfusion densities (2D), vessel surface areas and volumes (both 3D) were similar between control ($33.45\% \pm 1.16$; $42.84 \text{ mm}^2 \pm 11.83$; $0.18 \mu\text{m}^3 \pm 0.06$) and interventional eyes ($33.5\% \pm 4.18$; $40.39 \text{ mm}^2 \pm 9.99$; $0.17 \mu\text{m}^3 \pm 0.05$) (all $P > 0.25$). Following periocular anaesthesia, perfusion density was $31.72\% \pm 3.95$ in treated eyes, making it a significant intra-group decrease ($P < 0.032$), while the intra-group decrease in 3D vessel parameters was statistically insignificant ($38.55 \text{ mm}^2 \pm 8.24$; $0.16 \mu\text{m}^3 \pm 0.04$, both $P \geq 0.38$). In control eyes, all three vessel parameters remained relatively stable ($34.81\% \pm 3.08$; $44.79 \text{ mm}^2 \pm 9.86$; $0.19 \mu\text{m}^3 \pm 0.05$) (all $P > 0.25$). Following periocular anaesthesia, all three parameters demonstrated significant inter-group differences (all $P < 0.003$).

In interventional and control eyes both before and following periocular anaesthesia, perfusion density (2D) correlated moderately or strongly with vessel surface area and vessel volume (both 3D) (all $r^2 > 0.67$, all $P < 0.005$). The intra-group differences in perfusion density (Δ perfusion density) correlated strongly with the intra-group differences in vessel surface area (Δ vessel surface area) and vessel volume (Δ vessel volume) in both groups (all $r^2 > 0.75$, all $P < 0.005$). Complete correlation coefficients are shown in Table S2.

3.3.2 | Imaging artifacts

Motion artifacts occurred frequently in both groups and measurement time-points (although often only minor or moderate), yet Free-of-Motion-Artifact (FoMA) score was slightly higher in control eyes (pre-intervention: 2.07 ± 1.57 , postintervention 1.77 ± 1.2) than interventional eyes (pre-intervention: 1.6 ± 1.28 , postintervention: 1.33 ± 1.4) (both $P > 0.13$). Examples of study participants for each score are shown in Figure 4.

No relevant correlation was found between FoMA score and any of the three assessed vessel parameters at any measurement time-point (all $r^2 < 0.29$, all $P > 0.12$).

Generally, mean signal strength was on a high level throughout groups and measurement time-points. Before anaesthetic injection, signal strength was similar in control and interventional eyes (control eyes: 8.67 ± 1.45 ; interventional eyes: 8.63 ± 1.28). Following periocular anaesthesia, however, signal strength was higher in controls than interventional eyes (control eyes: 9.33 ± 0.83 ; interventional eyes: 8.27 ± 1.46) ($P < 0.005$). In both groups before and during periocular anaesthesia, all three perfusion parameters correlated at least moderately with signal strength (all $r^2 > 0.61$, all $P < 0.005$).

Another OCTA image artifact repeatedly observed in our patients undergoing cataract surgery is absorption of laser light by clouded lenses and subsequent signal deprivation/

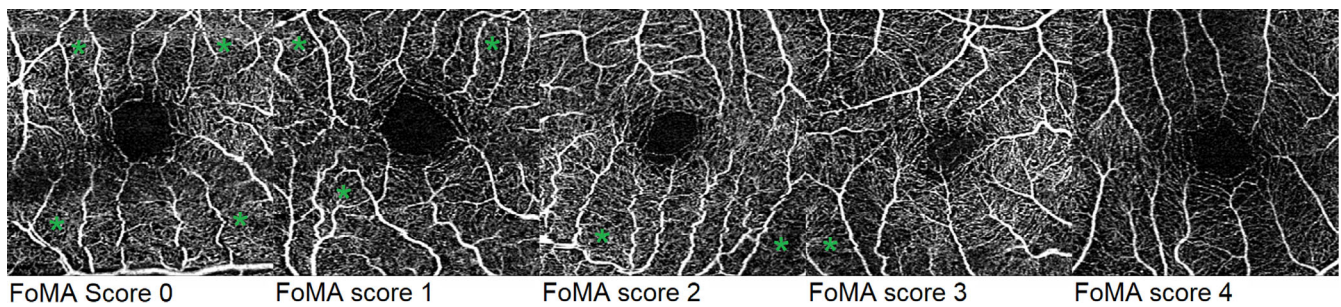


FIGURE 4 Free-of-Motion-artifact scoring from 0 to 4. Exemplary presentation of OCTA images with motion artifacts in all quadrants and score 0 (0), in three quadrants and score 1 (1), in two quarters and score 2 (2), in one quarter and score 3 (3) as well as an OCTA image from a study participant without motion artifacts and score 4 (4). Regions of motion artifacts are marked green.

FIGURE 5 Signal Extinction due to lens clouding. Example of OCTA image of a study participant with distinct focal lens clouding and subsequent laser light absorption and signal extinction (signal strength 10); display of original perfusion image, map and trace.

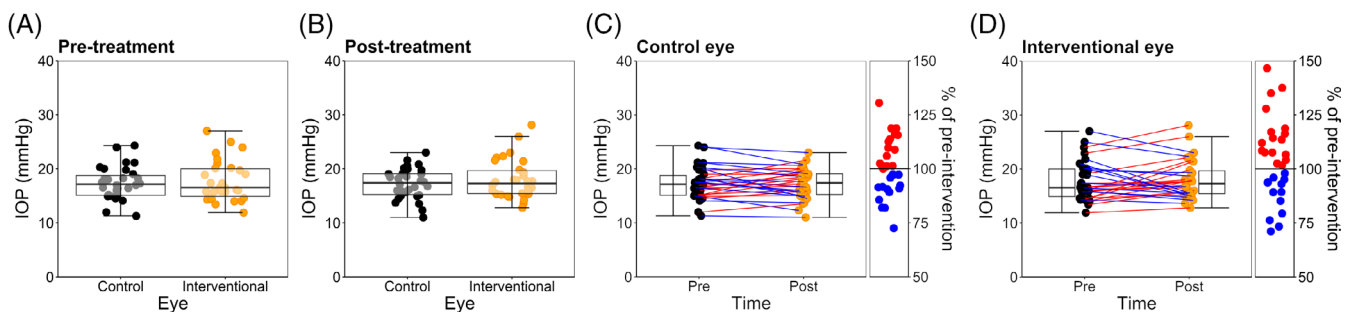
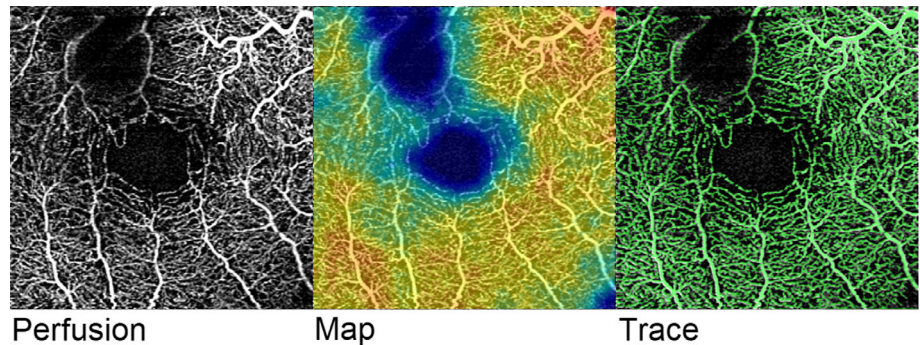


FIGURE 6 Intraocular pressure in the control eyes and the interventional eyes before and after sub-Tenon's block. Box and whisker plots showing IOP values (mmHg) in the control and interventional eyes before (A) and after (B) application of sub-Tenon's block. Box and whisker plots showing IOP changes before and after application of sub-Tenon's anaesthesia in the control (C) and interventional eyes (D).

extinction, likely affecting perfusion assessment/quantification. A typical example is shown in Figure 5.

Like many other OCTA devices, Zeiss Cirrus offers a projection artifact removal algorithm. However, in our study, OCTA raw data were exported from the device to be further postprocessed using our custom Matlab script. In these original data, the manufacturer's algorithm was not supported. Thus, projection artifacts removal was not performed.

3.4 | Intraocular pressure and arterial blood pressure

Before periorbital anaesthesia, mean IOP in interventional and control eyes were similar (17.69 ± 3.7 mmHg

[range from 11.9 to 27.0 mmHg] and 17.37 ± 3.01 [range from 11.3 to 24.3 mmHg], respectively; $P = 0.97$). Following anaesthetic injection, mean IOP remained stable (interventional: 18.02 ± 3.63 mmHg, $P = 0.52$; control: 17.26 ± 2.83 mmHg, $P = 0.80$; [inter-group difference: $P = 0.48$]). Data are shown in Figure 6 and Table S1.

IOP was comparable in both groups before and after the anaesthetic block. No significant changes were observed.

Mean systolic and diastolic BP increased slightly following periorbital anaesthetic application (from 145.37 ± 22.41 mmHg and 85.60 ± 13.89 mmHg to 149.90 ± 26.64 mmHg [$P < 0.05$] and 86.00 ± 13.41 mmHg [$P = 0.79$], respectively). No correlation was found between perfusion parameters and IOP or arterial BP after anaesthetic injection (all $P > 0.5$) in interventional eyes.

4 | DISCUSSION

4.1 | Feasibility of volume-rendered optical coherence tomography for retinal perfusion assessment/monitoring in a surgical setting

In this feasibility study, we sought for proof-of-concept for applicability of volume-rendered OCTA for 3D assessment and quantification of the retinal vasculature at the micron-level in a surgical setting and ultimately to explore the potential for intraoperative use. To this purpose, we enrolled patients undergoing periocular anaesthesia, since published evidence suggests a reduction in ocular blood flow. [28–30] In our study, imaging procedures under real-life conditions in a surgical theatre were overall successful. In all patients and eyes, it was possible to acquire images of sufficient quality to be postprocessed before and during the intervention. Thus, we demonstrated the capability to obtain 3D OCTA-based retinal vasculature assessment in challenging surgical settings safely and noninvasively. Since we were able to perform repeated imaging over a period of time, we further supported that it is possible to use this imaging technology to continuously depict vessel size changes at the micron-level and hence to monitor retinal perfusion during ocular procedures.

Beside our custom 3D vessel size quantification algorithm, our analyses involved the conventional 2D vessel quantification algorithm by AngioPlex Metrix, allowing for direct comparison of the two methods. This first-ever lineup of the two techniques revealed close correlation between perfusion data, advocating reliability of the two quantification modalities. Given the custom method's much more sophisticated principle of work, these findings support the rationale that the technique depicts and quantifies retinal vasculature in much more detail and accuracy (at the micron-level), whereas the conventional method does so only very vaguely (percentage of moving pixels).

Striving to identify possible disruptive factors associated with the imaging process, we marked off motion artifacts and signal deprivation/extinction phenomena in our OCTA images, as well as differences in signal strength as displayed by the device. We developed a motion-artifact score, graded all images accordingly and screened for correlations between 2D/3D OCTA-derived vessel data and this score, as well as with signal strength. No correlation was found between both 2D and 3D perfusion parameters and our motion artifact score, which may allow for the conclusion that both quantification techniques are robust against this type of artifact. In contrast, we found a positive correlation between all three perfusion parameters and signal strength. Although in

our cohort signal strengths were generally on high levels that could be considered acceptable, it appears suggestive that the differences in signal strength may have influenced perfusion quantification at least partially. Lim and colleagues reported on the dependence of 2D perfusion density measurement outcomes on signal strengths. [11] In view of our findings, it appears probable that volume-rendering of OCTA data unfortunately cannot overcome this vulnerability.

Since lens clouding was likely more pronounced on the interventional side (patients were scheduled for cataract surgery), it is conceivable that signal deprivation was more prevalent on that side as well, likely affecting perfusion quantification. Interestingly, obvious focal signal extinction is not necessarily reflected in signal strength as displayed by the device (see Figure 6 for an example of pronounced signal extinction and maximum signal strength), which makes the value of signal strength indication questionable and the grading, interpretation and handling of signal deprivation/extinction phenomena difficult.

Retinal imaging in a surgical setting depends on many unknown variables possibly affecting imaging accuracy, for example, the correct positioning of the patient's head on the device, unsteady fixation, or dry ocular surface. While signal deprivation and motion artifacts hence appear almost inevitable in monitoring cataract patients in a dynamic surgical setting with current OCTA technology, projection artifacts can principally be removed using software algorithms. In our study, this was not performed since the manufacturer's software does not allow for combined raw data export and projection artifact removal. This could be considered a further caveat to the imaging method being investigated here. In this context, however, it is noteworthy that each OCTA system uses a different technology for projection artifact removal. So far, no consensus on a generally acceptable procedure or threshold for a valid artifact level has been reached. As complete raw data is provided, the measured values are readily adjustable at any time which should aid in future or further in-depth data analysis.

4.2 | Effect of periocular anaesthesia on retinal blood flow

Regarding vessel size scrutiny, we first conducted analysis based on averaged 3D vasculature data from before and during periocular anaesthesia. This analysis showed significant postinjection inter-group differences, yet no significant intra-group differences. The lack of such differences could be explained by a possible masking effect due to averaging data obtained at different time-points

relative to the anaesthetic application. Therefore, we used a time-standardizing approach for our second examination. The results of this single-volume-based analysis suggest that both 3D vessel parameters decreased significantly within minutes after anaesthetic application in interventional eyes, whereas again no relevant changes could be observed in the fellow eyes. In our third analysis, we used only the qualitatively best available images before and during periocular anaesthesia. This analysis again revealed a decrease in 3D vessel data following anaesthetic injection, yet it was statistically insignificant. However, in this dataset, the time span between anaesthetic injection and imaging was relatively large in many cases, hence a more pronounced but transient vasoconstrictive effect may have been missed.

Periocular anaesthesia has been associated with a reduction in ocular blood flow and retinal vaso-occlusive events, yet the mechanism behind this phenomenon remained unclear. [16, 20] A direct compression of the retinal vessels as a result of intraocular pressure (IOP) spikes is unlikely, since sub-Tenon's anaesthesia does not appear to be associated with significant IOP changes. [28, 33] Instead, it is hypothesized that the anaesthetics exert a pharmacological vaso-constrictive effect, thereby diminishing retinal blood supply. [24, 27, 31, 32] Supporting this, anaesthetic agents have been shown to reduce nitric oxide-mediated relaxation of porcine ciliary arteries. [34] Compared with other anaesthetics, mepivacaine is considered to have the least pronounced vaso-constrictive effect, [35, 36] and we applied only 2 ml of mepivacaine solution 2%. Nonetheless and although likely confounded by imaging artifacts, our findings appear to confirm a possible reduction in retinal perfusion. No relevant changes in IOP were measured, which is consistent with previous reports. [28, 33] No correlation was found between postinterventional vessel parameters and IOP or arterial BP in the treated eyes. Considering this, an IOP-mediated compression of the ocular vessels or perfusion alterations caused by arterial BP fluctuations are unlikely. Our data appear to support the rationale of a direct pharmacological vasoconstrictive effect as the cause of the presumed reduction in retinal blood flow, seconding other investigators' recommendation to be cautious when using periocular anaesthesia, especially in patients with previously compromised ocular perfusion (e.g., in diabetic retinopathy). [24, 28]

4.3 | Implications for research

Follow-up studies with larger cohorts of patients and further evolved equipment allowing for continuous imaging and real-time perfusion quantification are necessitated to further explore the potential of 3D

OCTA for intraoperative use, as well as to investigate the precise effect of different periocular/intracameral/topical anaesthetic procedures on retinal blood flow in health and disease. Currently, we are projecting sequel studies involving a Zeiss OCTA prototype platform built into an operating microscope for true intraoperative imaging in patients with healthy retinas and ischemic retinopathies.

5 | CONCLUSION

In conclusion, our study demonstrates the feasibility of volume-rendered OCTA for providing 3D vasculature assessment in a challenging surgical setting. Our study further supports that using this technology is generally possible to continuously depict and quantify small changes in retinal vessel size at the micron-level and thus to monitor retinal perfusion during ocular procedures. The effect of signal strength and different types of artifacts on vasculature quantification is yet to be fully clarified. However, 3D OCTA appears principally viable for intraoperative use. Volume-rendered OCTA is a promising candidate to meet the need for a noninvasive and safe method for intraoperative retinal perfusion assessment.

AUTHOR CONTRIBUTIONS

Tim J. Enz and Peter M. Maloca contributed equally to this study. Tim J. Enz and Peter M. Maloca conceptualized the study. Tim J. Enz obtained ethical approval. Tim J. Enz and Anthia Papazoglou recruited patients and obtained informed consent. Tim J. Enz, Markus Tschopp, Marcel N. Menke, Ulrike Steitz and Anthia Papazoglou conducted surgical interventions and imaging procedures. Marcel N. Menke allocated resources for patient recruitment and imaging procedures. Peter M. Maloca and Nadja Inglin performed image postprocessing, volume-rendering and 3D vessel quantification. Hendrik P. N. Scholl allocated resources for image postprocessing, volume-rendering and 3D vessel quantification. Tim J. Enz and James R. Tribble performed data curation. Tim J. Enz, James R. Tribble and Pete A. Williams conducted statistical analysis and figure preparations. Tim J. Enz and Peter M. Maloca interpreted the data. Tim J. Enz, Peter M. Maloca and Pete A. Williams drafted the manuscript. Pete A. Williams allocated resources for data curation, statistical analysis, figure preparation and manuscript drafting. All authors reviewed the manuscript. All named authors take responsibility for the integrity of the work as a whole and have given their approval for this version of the manuscript to be published. The authors would like to acknowledge Melissa Jöe for assistance in

statistical analysis and Professor Rick Spaide for providing the graphical abstract figure.

FUNDING INFORMATION

Hendrik P. N. Scholl is supported by the Swiss National Science Foundation, National Center of Competence in Research Molecular Systems Engineering “Molecular Systems Engineering” and project funding in biology and medicine (“Developing novel outcomes for clinical trials in Stargardt disease using structure/function relationship and deep learning” #310030_201165), the Wellcome Trust (PINNACLE study), the Translational Research Acceleration Program Award by the Foundation Fighting Blindness (“Cone-based optogenetics for vision restoration” #TA-NMT-0621-0805-TRAP), and the Foundation Fighting Blindness Clinical Research Institute (ProgStar study). Pete A. Williams is supported by Karolinska Institutet in the form of a Board of Research Faculty Funded Career Position and by St. Erik Eye Hospital philanthropic donations, Vetenskapsrådet 2018-02124.

CONFLICT OF INTEREST

Peter M. Maloca is consultant of Zeiss Forum, Roche and Bayer UK and holds patents for speckle denoising and machine learning. Hendrik P. N. Scholl is member of the Scientific Advisory Board of: Apellis Switzerland GmbH, ARCTOS medical AG; Astellas Pharma Global Development, Inc./Astellas Institute for Regenerative Medicine; Biogen MA Inc.; Boehringer Ingelheim Pharma GmbH & Co; Gyroscope Therapeutics Ltd.; Janssen Research & Development, LLC (Johnson & Johnson); Novartis Pharma AG (CORE); Okuvision GmbH; Pharma Research & Early Development (pRED) of F. Hoffmann-La Roche Ltd; ReVision Therapeutics, Inc.; and Stargazer Pharmaceuticals, Inc. Hendrik P. N. Scholl is a paid consultant of: Gerson Lehrman Group; Guidepoint Global, LLC; Tenpoint Therapeutics Limited; and Third Rock Ventures, LLC. Hendrik P. N. Scholl is member of the Data Monitoring and Safety Board/Committee of Belite Bio and ReNeuron Group Plc/Ora Inc. and member of the Steering Committee of Novo Nordisk (FOCUS trial). Hendrik P. N. Scholl is co-director of the Institute of Molecular and Clinical Ophthalmology Basel (IOB) which is constituted as a nonprofit foundation and receives funding from the University of Basel, the University Hospital Basel, Novartis, and the government of Basel-Stadt. These arrangements have been reviewed and approved by the University of Basel (Universitätsspital Basel, USB) in accordance with its conflict of interest policies. Hendrik P. N. Scholl is principal investigator of grants at the USB sponsored by the following entities: Kinarus AG; Okuvision GmbH; and Novartis Pharma AG. Grants at USB are negotiated and administered by the institution (USB)

which receives them on its proper accounts. Individual investigators who participate in the sponsored project(s) are not directly compensated by the sponsor but may receive support from the institution for their project(s). The authors declare no conflict of interest. The funders had no role in the design of the study; in the collection, analyses, or interpretation of data; in the writing of the manuscript; or in the decision to publish the results.

ACKNOWLEDGEMENTS

Open access funding provided by Universitat Basel.

DATA AVAILABILITY STATEMENT

The data that support the findings of this study are available from the corresponding author upon reasonable request.

ETHICS STATEMENT

This observational study was conducted in accordance with the Declaration of Helsinki and was approved by the competent ethics committee (Ethikkommission Nordwest- und Zentralschweiz EKNZ, identification number 2019-01689).

CONSENT FOR PUBLICATION

Written informed consent was obtained from all patients after explanation of the nature and possible consequences of the study. All published data is anonymized.

ORCID

Tim J. Enz  <https://orcid.org/0000-0002-5211-7855>

REFERENCES

- [1] J. M. Googe, M. Bessler, J. C. Hoskins, J. H. Miller, *Ophthalmology* **1993**, *100*, 1167.
- [2] H. Terasaki, Y. Miyake, S. Awaya, *Am J Ophthalmol* **1997**, *123*, 370. [https://doi.org/10.1016/s0002-9394\(14\)70133-3](https://doi.org/10.1016/s0002-9394(14)70133-3).
- [3] H. Imai, A. Tetsumoto, H. Yamada, M. Hayashida, K. Otsuka, A. Miki, M. Nakamura, *Retin Cases Brief Rep* **2020**. <https://doi.org/10.1097/ICB.0000000000001091>.
- [4] H. Imai, A. Tetsumoto, S. Inoue, F. Takano, H. Yamada, M. Hayashida, K. Otsuka, A. Miki, S. Kusuhara, M. Nakamura, *Retina* **2020**. <https://doi.org/10.1097/IAE.0000000000002805>.
- [5] R. F. Spaide, J. G. Fujimoto, N. K. Waheed, S. R. Sadda, G. Staurengi, *Prog Retin Eye Res* **2018**, *64*, 1. <https://doi.org/10.1016/j.preteyeres.2017.11.003>.
- [6] J. Chua, R. Sim, B. Tan, D. Wong, X. Yao, X. Liu, D. S. W. Ting, D. Schmidl, M. Ang, G. Garhöfer, L. Schmetterer, *J Clin Med* **2020**, *9*, 1723. <https://doi.org/10.3390/jcm9061723>.
- [7] M. Pellegrini, A. Vagge, L. F. Ferro Desideri, F. Bernabei, G. Triolo, R. Mastropasqua, C. D. del Noce, E. Borrelli, R. Sacconi, C. Iovino, et al., *J Clin Med* **2020**, *9*, 1706. <https://doi.org/10.3390/jcm9061706>.
- [8] S. S. Ong, T. P. Patel, M. S. Singh, *J Clin Med* **2019**, *8*, 2078. <https://doi.org/10.3390/jcm8122078>.

- [9] M. C. Savastano, M. Rispoli, B. Lumbroso, L. Di Antonio, L. Mastropasqua, G. Virgili, A. Savastano, D. Bacherini, S. Rizzo, *Eur J Ophthalmol* **2021**, *31*, 514. <https://doi.org/10.1177/1120672120909769>.
- [10] R. Meyer-Schwickerath, T. Kleinwächter, R. Firsching, H. D. Papenfuss, *Graefes Arch Clin Exp Ophthalmol* **1995**, *233*, 783. <https://doi.org/10.1007/bf00184090>.
- [11] H. B. Lim, Y. W. Kim, J. M. Kim, Y. J. Jo, J. Y. Kim, *Sci. Rep.* **2018**, *8*, 12897. <https://doi.org/10.1038/s41598-018-31321-9>.
- [12] R. F. Spaide, *Retina* **2015**, *35*, 2181. <https://doi.org/10.1097/IAE.0000000000000764>.
- [13] R. F. Spaide, J. M. Klančnik, M. J. Cooney, L. A. Yannuzzi, C. Balaratnasingam, K. K. Dansingani, M. Suzuki, *Ophthalmology* **2015**, *122*, 2261. <https://doi.org/10.1016/j.ophtha.2015.07.025>.
- [14] M. Reich, M. Dreesbach, D. Boehringer, J. Schottenhamml, E. Gehring, H. P. Scholl, N. Inglin, H. Agostini, T. Reinhard, W. A. Lagrèze, et al., *Retina* **2021**, *41*, 1948. <https://doi.org/10.1097/IAE.0000000000003110>.
- [15] P. M. Maloca, R. F. Spaide, E. R. de Carvalho, H. P. Studer, W. Hasler, H. P. N. Scholl, T. F. C. Heeren, J. Schottenhamml, K. Balaskas, A. Tufail, et al., *Graefes Arch Clin Exp Ophthalmol* **2020**, *258*, 711. <https://doi.org/10.1007/s00417-019-04582-x>.
- [16] C. M. Kumar, H. Eid, C. Dodds, *Eye (London)* **2011**, *25*, 694. <https://doi.org/10.1038/eye.2011.69>.
- [17] R. M. Feibel, D. L. Guyton, *J Cataract Refract Surg* **2003**, *29*, 1821. [https://doi.org/10.1016/s0886-3350\(02\)01975-2](https://doi.org/10.1016/s0886-3350(02)01975-2).
- [18] H. Rüschen, F. D. Bremner, C. Carr, *Anesth Analg* **2003**, *96*, 273. <https://doi.org/10.1097/0000539-200301000-00054>.
- [19] I. H. Yusuf, T. H. Fung, M. Wasik, C. K. Patel, *Eye (Lond)* **2014**, *28*, 1375. <https://doi.org/10.1038/eye.2014.190>.
- [20] R. A. Fry, P. Ring, *Clin Exp Ophthalmol* **2008**, *36*, 196. <https://doi.org/10.1111/j.1442-9071.2008.01686.x>.
- [21] M. E. Zarzosa Martín, I. Roberts Martínez-Aguirre, N. Gajate Paniagua, E. Pérez-Salvador García, Transient central retinal artery occlusion after sub-tenon's anaesthesia: Is it a safe technique? in *Archivos Sociedad Española de Oftalmología (English ed.)*, Vol. 92 **2017**, p. e78. Amsterdam: Elsevier. <https://doi.org/10.1016/j.oftale.2017.06.010>.
- [22] R. M. H. Lee, J. R. Thompson, T. Eke, *Br J Ophthalmol* **2016**, *100*, 772. <https://doi.org/10.1136/bjophthalmol-2015-307060>.
- [23] D. Dragnev, D. Barr, M. Kulshrestha, S. Shanmugalingam, *Case Rep Ophthalmol* **2013**, *4*, 27. <https://doi.org/10.1159/000348729>.
- [24] K. Creese, D. Ong, S. S. Sandhu, D. Ware, C. Alex Harper, S. H. Al-Qureshi, S. S. Wickremasinghe, *Clin Exp Ophthalmol* **2017**, *45*, 598. <https://doi.org/10.1111/ceo.12945>.
- [25] W. Henein, A. Wilson-Pogmore, F. Imrie, *Am J Ophthalmol Case Rep* **2020**, *20*, 100925. <https://doi.org/10.1016/j.ajoc.2020.100925>.
- [26] C. Pham, A. Boo, S. K. H. Chew, M. Okada, *Clin Exp Ophthalmol* **2019**, *47*, 1206. <https://doi.org/10.1111/ceo.13597>.
- [27] R. O'Day, C. A. Harper, S. S. Wickremasinghe, *Clin Exp Ophthalmol* **2019**, *47*, 141. <https://doi.org/10.1111/ceo.13353>.
- [28] P. Pianka, H. Weintraub-Padova, M. Lazar, O. Geyer, *J Cataract Refract Surg* **2001**, *27*, 1221. [https://doi.org/10.1016/s0886-3350\(01\)00797-0](https://doi.org/10.1016/s0886-3350(01)00797-0).
- [29] R. Watkins, B. Beigi, M. Yates, B. Chang, E. Linardos, *Br J Ophthalmol* **2001**, *85*, 796. <https://doi.org/10.1136/bjo.85.7.796>.
- [30] M. Coşkun, M. C. Dağlioğlu, R. Davran, N. Ilhan, O. Ilhan, E. Ayhan Tuzcu, E. Ayintap, U. Keskin, H. Oksüz, *Can J Ophthalmol* **2014**, *49*, 141. <https://doi.org/10.1016/j.jcjo.2013.10.004>.
- [31] F. K. Chen, *Clin Exp Ophthalmol* **2017**, *45*, 565. <https://doi.org/10.1111/ceo.13010>.
- [32] O. Findl, S. Dallinger, R. Menapace, G. Rainer, M. Georgopoulos, B. Kiss, L. Schmetterer, *Am J Ophthalmol* **1999**, *127*, 645. [https://doi.org/10.1016/s0002-9394\(99\)00066-5](https://doi.org/10.1016/s0002-9394(99)00066-5).
- [33] A. Alwitry, Z. Koshy, A. C. Browning, W. Kiel, R. Holden, *Eye (Lond)* **2001**, *15*, 733. <https://doi.org/10.1038/eye.2001.239>.
- [34] P. Meyer, J. Flammer, T. F. Lüscher, *Invest Ophthalmol Vis Sci* **1993**, *34*, 2730.
- [35] H.-J. Sung, S.-H. Ok, J.-Y. Sohn, Y. H. Son, J. K. Kim, S. H. Lee, J. Y. Han, D. H. Lim, I.-W. Shin, H.-K. Lee, Y. K. Chung, M. J. Choi, J. T. Sohn, *J Biomed Biotechnol* **2012**, *2012*, 170957. <https://doi.org/10.1155/2012/170958>.
- [36] H. H. Lindorf, *Oral Surg Oral Med Oral Pathol* **1979**, *48*, 292. [https://doi.org/10.1016/0030-4220\(79\)90026-4](https://doi.org/10.1016/0030-4220(79)90026-4).

SUPPORTING INFORMATION

Additional supporting information can be found online in the Supporting Information section at the end of this article.

How to cite this article: T. J. Enz, P. M. Maloca, M. Tschopp, M. N. Menke, J. R. Tribble, P. A. Williams, N. Inglin, U. Steitz, H. P. N. Scholl, A. Papazoglou, *J. Biophotonics* **2022**, 202200169. <https://doi.org/10.1002/jbio.202200169>